Droplet Collision Dynamics in Turbulence

Submitted in partial fulfillment of
the requirements for the award of the degree of

BS-MS
in
Natural Sciences

Submitted by

Lokahith Narendra Agasthya   (Reg. No. 20131034)

Under the guidance of
Rama Govindarajan and Samriddhi Sankar Ray

ICTS Bengaluru

IISER PUNE

Indian Institute of Science Education and Research

DR. HOMI BHABHA ROAD

Pune, Maharashtra, India – 411 008

March 2018

Certificate

This is to certify that this thesis entitled Droplet Collision Dynamics in Turbulence submitted towards the partial fulfillment of the BS-MS dual degree programme at the Indian Institute of Science Education and Research Pune represents original research carried out by Lokahith Narendra Agasthya at the International Centre for Theoretical Sciences, Tata Institute of Fundamental Research, Bengaluru, under the supervision of Prof. Rama Govindarajan and Prof. Samriddhi Sankar Ray during the academic year 2017-2018.
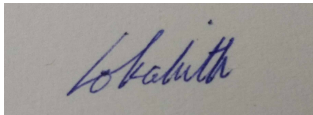
Lokahith Narendra
Agasthya
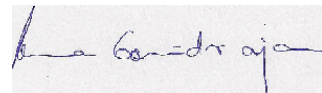
Prof. Rama
Govindarajan

Declaration

I hereby declare that the matter embodied in the report entitled Droplet Collision Dynamics in Turbulence are the results of the investigations carried out by me at the International Centre for Theoretical Sciences, Tata Institute of Fundamental Research, Bengaluru, under the supervision of Prof. Rama Govindarajan and Prof. Samriddhi Sankar Ray and the same has not been submitted elsewhere for any other degree.
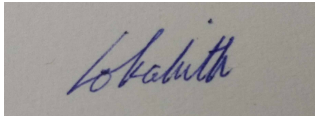
Lokahith Narendra
Agasthya
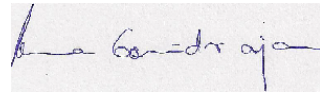
Prof. Rama
Govindarajan

Acknowledgments

Since this document is the defining academic output of my 5 years affiliated to IISER Pune, I would like to take this opportunity to thank all those who helped define this long and constructive period of my life.

Firstly, I am eternally grateful to my parents, my mother Manasa for her constant encouragement, positivity and energy, and my father Anantha, for his guidance, support and his proactive interest in my academic life. My sisters Greeshma and Poshini have been like two pillars throughout this journey and I am sure they will continue to be for the rest of my life. Through the highs and lows of the last five years, I was able to instantaneously multiply my joy and divide my sorrows by sharing it with them.

College years being the best years of ones life is perhaps the greatest example of a cliche that is true. My life would have been drab and dull these past five years but for the intervention of my dear friends. The names of the gentlemen and ladies who have added colour to my life would take several pages to list, not to mention valuable time just before the deadline for thesis submission. It is harder though, to leave out the names of a few bosom friends in a document of such significance. It is equally hard as well, to pick out the names of just a few friends to especially acknowledge in this space. However, it is a task I am compelled to undertake for the significant influence these friends have had on me. Naven Venkat, Bharath Krishnan, Karthik Prabhu and Sruti Ramesh have in turn been stern with me, coddled me, left me to my devices and held my hand to guide me, as and when it was in my interest to do so, and to them I am indebted for their friendship, time and love.

The 5th year project is an arduous assignment and requires discipline and focus to conduct research. In this pursuit, I moved away from my abode of IISER Pune to ICTS Bengaluru, where I was welcomed warmly and where I quickly settled in the dear company of Sushmita Singh, Girish Muralidhara, Nidhi Sudhir and Mohit Gupta, to name of the few friendships that have blossomed in the past year of my life.

In the academic sphere, I am very grateful to Prof. Tarun Souradeep at IUCAA, Pune, for being my guide during a semester long project and starting me off on the techniques of computational physics. Prof. Rama Govindarajan and Prof. Samriddhi Sankar Ray, the co-guides for my final year project have been helpful and understanding throughout my stint at ICTS, while at the same time demanding in terms of work, pushing me to work to the best of my ability. I am extremely thankful for their guidance and the time they have often spared to lend me advice on all things academic. It was during

this period as well, that I recaptured my love for science that had deserted me mid-way through my life at IISER, with the ennui of coursework and exams. This rekindling of my old passion was in no small part due to the example set by Prof. Rama and Prof. Samriddhi.

Playing the part of both, an academic advisor as well as a good friend and companion, the work done by me over the past year at ICTS would be impossible without Jason Picardo's constant voice in my ear. Several discussions on science, history, books, fluid dynamics, climate sciences and a multitude of other topics were the perfect antidote to the occasional boredom of life at ICTS. His passion and enthusiasm for research was contagious and is a big reason for me to continue along the path of academia and pursue a PhD after my Masters programme.

I am thankful to the Department of Science and Technology, Government of India for awarding me with the INSPIRE SHE fellowship for the duration of my Masters. Lastly, I am also thankful to all the staff involved at ICTS and IISER, from the director to the house-keeping staff for all their efforts towards making these two institutions among the finest in the country and institutes which will always be close to my heart.

Abstract

The study of the collision dynamics of small spherical particles suspended in a fluid has several applications, in industry as well as science. Of particular interest to this study is the application to cloud droplets in the atmosphere.

The Cloud Droplet Growth Bottleneck problem is an attempt to explain the rapid growth of cloud droplets from the size of a few microns to raindrops which are a few millimetres in diameter. The collision and consequent coalescence of droplets is a major factor in this rapid growth and fluid turbulence is touted to explain the enhancement of collisions of droplets. In this study, we aim to explore the roles of vortices, or regions of fluid flow which are roughly circular in direction, in creating collisions between particles suspended in flow similar to atmospheric flows and their impact on the growth of droplets.

Contents

Chapter 1

Introduction

Overview

The work done in this study can be delineated into two primary fields of research - fluid dynamics and cloud microphysics. Several aspects of these two fields have been studied in detail with the ultimate aim of simulating growing cloud droplets in a turbulent atmosphere to gain a clear understanding of rain formation in warm clouds (clouds without ice).

This document is a detailed report of the work that has been done by the author under the guidance of Prof. Rama Govindarajan and Prof. Samridhhi Sankar Ray along with Dr. Jason Picardo at the International Centre of Theoretical Sciences (ICTS), Bengaluru. The project has also entailed using the high performance computing centre at ICTS and in the process, has taught the author valuable skills in computational physics.

The main problem being tackled here is to understand the rapidity of onset of rain in warm clouds (the statement of the problem will be discussed in detail later). This work is also generally applicable to problems of relevance to industry and science where spherical, massive particles with small radii are suspended in a fluid and collisions between these suspended particles play an important role. The manufacture of powder and formation of planets by accretion of dust on to planetesimals are two of the several examples of such applications.

An Outline of the Thesis

The thesis proceeds as follows. Chapter 2 describes the relevant microphysics of clouds, ie., how cloud droplets grow via a) condensation and b) collisions during gravitational settling. Following this, the chapter discusses the state-

ment of the so called cloud droplet growth bottleneck problem, a failure in explaining the observed rapidity of onset of rain in warm clouds.

In the Chapter 3, the fundamentals of fluid dynamics of the study are described in detail with an introduction to the simplified Maxey-Riley equation that describes the dynamics of a spherical particle suspended in a fluid. The consequences of the Maxey-Riley equation for the positions and velocities of the particles in various regimes will also be discussed.

Chapter 4 merges these two threads and describes the role of fluid dynamics and turbulence in clouds. A summary of the work done during the period of this study along with a few results are also discussed.

Chapter 5 discusses these results both, independently and in the context of other work currently being undertaken by the fluid dynamics group at ICTS to which the author has contributed. Following this, the applicability of the work is discussed and the outlook for continuing work along the same lines is touched upon.

The author hopes that the reader finds this document enjoyable and informative.

Chapter 2

Cloud Microphysics

2.1 Clouds - An Introduction

A cloud is a collection of tiny water droplets that range in radius from a few microns up to few millimetres. Droplets greater than 100 microns are classified as drizzle droplets while droplets greater than 0.5 mm are classified as rain droplets as these droplets tend to fall out of the cloud due to their larger free-fall terminal velocities. They either reach the ground as rain, evaporate before they reach the ground or are not allowed to fall by stronger convective up-drafts below the cloud.

2.2 Cloud Droplet Activation

The formation of cloud droplets requires a solid particle (or aerosol) on to which water vapour can condense at high enough concentrations of water vapour in the atmosphere. This process of condensation of water on to an aerosol is known as activation and the aerosol particle is called a cloud condensation nucleus (CCN). CCNs come in a variety of sizes (ranging from a few nanometre to 100s of nanometre), shapes and chemical compositions. The composition of CCNs play an important role in their activation with hygroscopic CCNs being activated more easily.

Aerosols are essential for condensation of water vapour. Spontaneous condensation of water vapour requires relative humidity of several hundred percent, which is never observed in the atmosphere. Aerosol activation usually takes place at a relative humidity of 98-102 %, which are routinely observed in the atmosphere. Thus, in temperatures too high for formation of ice, activation of CCNs is the only way cloud droplets are formed in the atmosphere.

Once activated, the resulting cloud droplets are a few microns in diameter

and are spherical in shape. These minute droplets grow and combine to eventually become rain drops, if and when conditions are favourable. [1]

2.3 Growth of Cloud Droplets

2.3.1 Condensation Growth of Cloud Droplets

In their initial stages, cloud droplets grow almost solely by condensation of water vapour on to the surface of the droplet, thus increasing the volume of the droplet. To understand this process, we consider a single droplet in a homogenous, isotropic environment with a constant temperature and concentration of water vapour (relative humidity slightly greater than 100%).

Water Vapour Concentration at the Droplet Surface

To begin with let the initial radius a_0 of the droplet be 2 microns and the temperature of the droplet T_d be equal to the ambient temperature T. At the surface of the droplet, due to the presence of an interface between water and air, there is constant evaporation and condensation of water with a local equilibrium set-up. While studying the equilibrium characteristics of spherical droplets over a micron in radius, we can ignore curvature effects (dependence on radius a) and solute effects (dependence the chemical nature of the condensation nucleus).

This vapour density at the surface (ρ_{va}) is merely given by the saturation vapour density over bulk water. This is the well known Clasius-Clapeyron equation

$$\rho_{va} = \frac{e^{\frac{L}{R_\nu}\left(\frac{1}{273.15} - \frac{1}{T_d}\right)}}{R_\nu T_d} * 611 [\text{kg m}^{-3}] \tag{2.1}$$

Here, the latent heat of condensation of water L is assumed to be constant over the given temperature range, giving the simple exponential form. R_ν is the universal gas constant for water vapour and 611 Pa is an experimentally well measured value of equilibrium partial pressure of water vapour at 273.15 K. T_d is in Kelvin.

Thus, the equilibrium concentration of water vapour at the surface of the droplet is different from the background concentration. This leads to a concentration gradient. When the relative humidity is greater than 100%, the background water vapour concentration is greater than that at the surface of the droplet. This leads to diffusion of water vapour towards the droplet and thus, condensation on to the droplet by Le Chatlier's Principle.

The Diffusion Equation

There is diffusion of water vapour towards the droplet due to the density difference between the surface of the droplet and the background. The density profile of the vapour will follow the diffusion equation:

$$\frac{\partial \rho_v}{\partial t} = D \nabla^2 \rho_v \qquad (2.2)$$

where ρ_v is vapour density (function of space and time) and D is molecular diffusivity of water vapour in air. The boundary conditions are $\rho_v(\infty, t) = \rho_v$ where ρ_v is the given or measured ambient vapour density and $\rho_v(a, t) = \rho_{va}$, which can be calculated from equation (2.1).

We solve the Diffusion equation (2.2) assuming isotropic vapour density distribution. The solution with the given boundary conditions is a standard result and is given by

$$\rho_v(r, t) = \rho_v + (\rho_{va} - \rho_v)\frac{a}{r}\left[1 - \mathrm{erf}\left(\frac{r - a}{2\sqrt{Dt}}\right)\right] \qquad (2.3)$$

Here, erf (x) is the error function defined by erf $(x) = \frac{2}{\sqrt{\pi}} \int_0^x e^{-t^2}\, dt$. From this expression, the flux of vapour into the droplet surface is given by

$$-D\left(\frac{\partial \rho_v}{\partial r}\right)_{r=a} = D\left(\frac{\rho_v - \rho_{va}}{a}\right)\left(1 + \frac{a}{\sqrt{\pi Dt}}\right) \qquad (2.4)$$

For time $t >> t_c = \frac{a^2}{\pi D}$. the final term in the above expression will be negligible. For typical atmospheric and droplet conditions, $t_c \approx 10^{-6}$ seconds which is much smaller than typical times scales of diffusion. Thus, we can drop this term and what survives is a time independent expression. We could have arrived at the same expression from the steady-state diffusion equation

$$D\nabla^2 \rho_v = 0 \qquad (2.5)$$

So, the density flux of vapour at the droplet surface is simply

$$D\frac{(\rho_v - \rho_{va})}{a}$$

The condensation of water vapour on to the droplet can be treated as an instantaneous process since, as stated previously, changes in vapour density in the atmosphere happen slowly, over much larger time scales than the condensation of water over the droplet. Thus, we can assume that any vapour that diffuses towards the droplet immediately condenses. This is known as the quasi-steady approach. The radius a can be treated as a constant in

calculations and the relevant equations will hold at each moment of time for each a.

So, if we integrate the incoming flux over the volume, we get mass flux of vapour which is equal to the change in mass of the droplet. If we denote by m, the mass of the droplet,

$$\frac{dm}{dt} = 4\pi a^2 D \frac{(\rho_v - \rho_{va})}{a} \tag{2.6}$$

giving

$$\frac{dm}{dt} = 4\pi a D (\rho_v - \rho_{va}) \tag{2.7}$$

Thermodynamics of the System

When water condenses on to the droplet, there is an associated release of latent heat of condensation. This causes an increase in the temperature of the droplet. If we assume that the atmosphere is an infinite bath of temperature T, then the temperature of the droplet T_d increases with condensation of water and reduces by transport of heat away from the droplet.

We can once again use the diffusion equation to model the flow of heat away from the droplet. With arguments identical to the previous section (skipped here for brevity), we obtain for the flow of heat Q

$$\frac{dQ}{dt} = 4\pi a K (T - T_d) \tag{2.8}$$

K is the thermal conductivity of air.

When the mass of the droplet changes due to condensation of water on it, there is release of latent heat associated with it. We know that latent heat is proportional to the change in mass. The thermodynamic equation for the droplet will thus be

$$mc\frac{dT_d}{dt} = L\frac{dm}{dt} + 4\pi a K (T - T_d) \tag{2.9}$$

where m is mass of the droplet, c is the specific heat of liquid water and L and K have already been defined. The last term is a direct substitution from equation (2.8).

Substituting for change of mass from equation (2.7) and writing the mass of the droplet as volume times density, we have

$$\frac{4}{3}\pi a^3 \rho_l c \frac{dT_d}{dt} = 4\pi a D L (\rho_v - \rho_{va}) - 4\pi a K (T_d - T) \tag{2.10}$$

with ρ_l being the density of liquid water. Simplifying for numerical integration, we get

$$\frac{dT_d}{dt} = \frac{3LD}{a^2\rho_l c}(\rho_v - \rho_{va}) - \frac{3K}{a^2\rho_l c}(T_d - T) \tag{2.11}$$

Growth of the Droplet

Re-writing the mass change equation (2.7) as

$$\frac{dm}{dt} = \rho_l 4\pi a^2 \frac{da}{dt} = 4\pi a D(\rho_v - \rho_{va}) \tag{2.12}$$

we have

$$\frac{da}{dt} = \frac{D}{a\rho_l}(\rho_v - \rho_{va}) \tag{2.13}$$

The growth of the droplet slows down as the droplet gets bigger. Again, it is important to keep in mind that ρ_{va} is a function of the temperature of the droplet, the exact form given by equation (2.1)

For the system under consideration, we need to solve equations (2.11) and (2.12) simultaneously by numerical methods with ambient vapour density ρ_v and ambient temperature T treated as given constants. Several attempts were made by the author to add simplifying assumptions to the equations and make it more analytically tractable. However, these attempts yielded no luck in making the equations analytically pliable.

There are a few characteristics of the growth of the droplet that can be stated by looking at the equations

1. Since $\frac{da}{dt} \sim a^{-1}$, smaller drops grow faster than larger drops

2. Since $\frac{da}{dt} \sim -\rho_{va}$ and ρ_{va} as given by equation (2.1) increases with increase in T_d, hotter drops grow slower than colder drops. (Or if their temperature is high enough, they can shrink by evaporation) [1, 2]

The equations were solved numerically for two cases, assuming zero release of latent heat (which corresponds to a case where the droplet is in constant heat equilibrium with the surroundings) and non-zero latent heat.
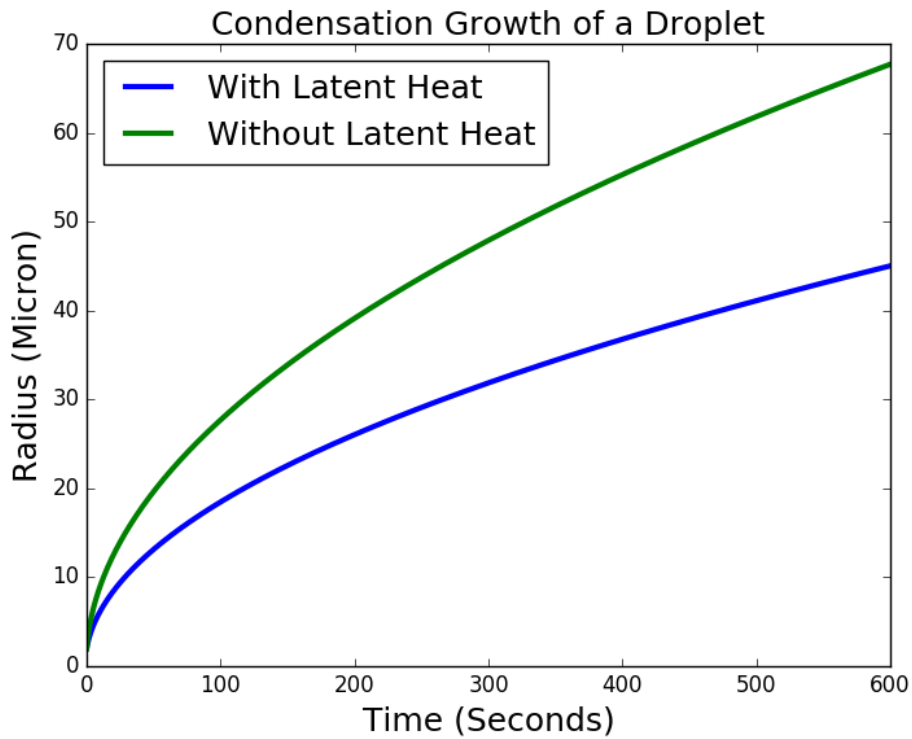
Figure 2.1: Condensation growth of a droplet with latent heat $L = 0$ and $L = 2.5 \times 10^6$ J kg^{-1} with a constant supersaturation of 2% and constant ambient temperature of $273\,\mathrm{K}$ for a short run of $600\,\mathrm{s}$ or 10 mins.
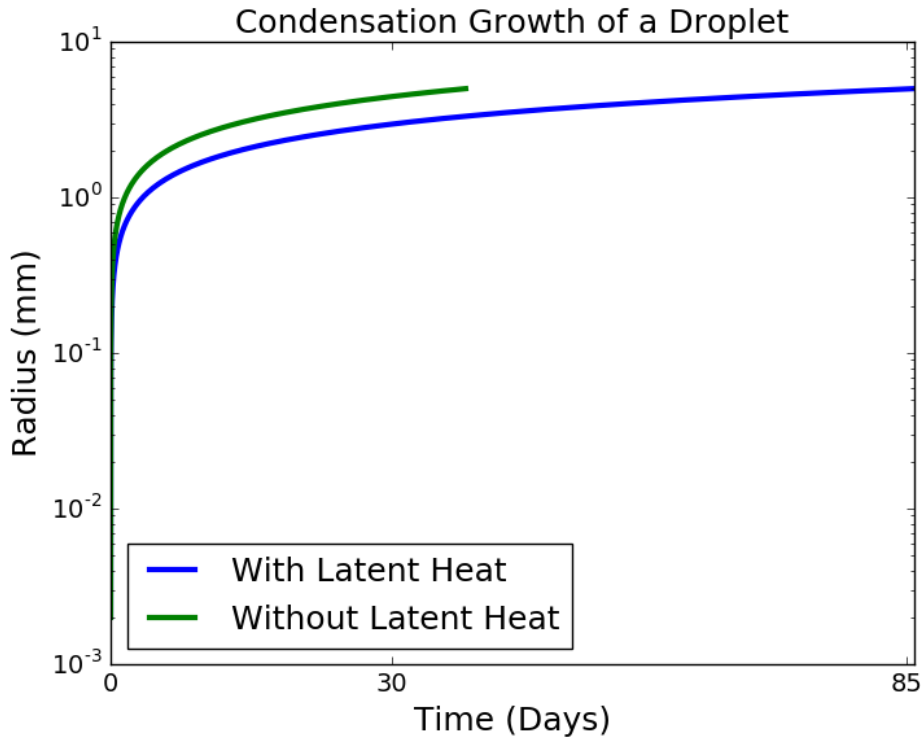
Figure 2.2: Semi-log plot of condensation growth of a droplet until it reaches a size of 5 mm with the same conditions as above. Even under idealised conditions, this takes several weeks.

2.4   Growth by Gravitational Settling

Since small drops ($\sim 2\,\mu\text{m}$) grow rapidly compared to larger drops by condensation, activated cloud droplets initially grow chiefly by condensation of water vapour on to the droplet. However, once they reach larger sizes, their large sizes and the limited amount of water vapour present in the atmosphere (having constant water vapour density is an idealisation), these droplets need another way to quickly grow and form rain-drops.

The other way droplets grow is by coalescence of small drops to form larger drops. This occurs chiefly by droplets falling under gravity at different speeds due to difference in their masses, and hence sizes.

Droplets have a downward 'terminal velocity' v_t when falling under grav-

ity, which is derived from the well-known Stokes law for drag on a sphere.

$$v_t = \frac{2a^2 \rho_p}{9\nu\rho_f} g \tag{2.14}$$

where ρ_p is the density of the particle, which is water in this case. ρ_f is the density of the fluid (air), ν is the kinematic viscosity of air, a is the radius of the sphere and g is acceleration due to gravity.

To estimate the rate of growth of a typical droplet by gravitational settling, assume a sea of droplets with radius of $10\,\mu m$ (the typical radius until where condensation growth is rapid and hence dominant) and a number fraction N close to the typical measured value of $4 \times 10^8\,\text{droplets/m}^3$. In this scenario, the coalescence of any 2 droplets by a chance event would create a droplet of radius $2^{\frac{1}{3}}*10\,\mu m$ ($\approx 12.6\,\mu m$).

This droplet would thus fall faster than the other droplets and collide with more droplets, leading it to grow even larger. However, it is observed that these drops initially have a very low collision efficiency. The collision efficiency increases with increase in difference in radii between two droplets. Let us denote by ϵ, the efficiency of collision of droplets, ie., the probability that two droplets who have an overlap coalesce to form a bigger droplet.

Let a_b denote the radius of the big droplet and v_b denote its velocity while a_0 denotes the radius of the other droplets ($10\,\mu m$ in this case) and v_0 denotes the terminal velocity of a droplet of radius a_0. In unit time, the large drop sweeps a cylinder of radius a_b as it falls and collisions happen with all droplets which overlap with this sphere. Thus, any droplet in a cylinder of radius $a_b + a_0$ just under the droplet will collide with the large drop. We can write

$$\frac{dV}{dt} = \epsilon N \pi (a_b + a_0)^2 (v_b - v_0)(\frac{4}{3}\pi a_0^3) \tag{2.15}$$

V denotes volume of the big droplet. Strictly, the collision efficiency ϵ is a function of a_b

Re-casting this in terms of radius, we get

$$\frac{da_b}{dt} = \epsilon \frac{(a_b + a_0)^2 (v_b - v_0)}{3a_b^2} \tag{2.16}$$

The relative velocity $(v_b - v_0)$ can be rewritten using equation (2.14), thus giving

$$\frac{da_b}{dt} = \epsilon \frac{(a_b + a_0)^2}{3a_b^2} v_0 \left(\frac{a_b^2}{a_0^2} - 1 \right) \tag{2.17}$$

This equation can be solved either numerically or analytically to give an estimate for growth by gravitational settling. We can take the efficiency of

collision 'ϵ' to be the maximum possible value to obtain a lower limit on how quickly a given droplet can grow to become a rain drop.
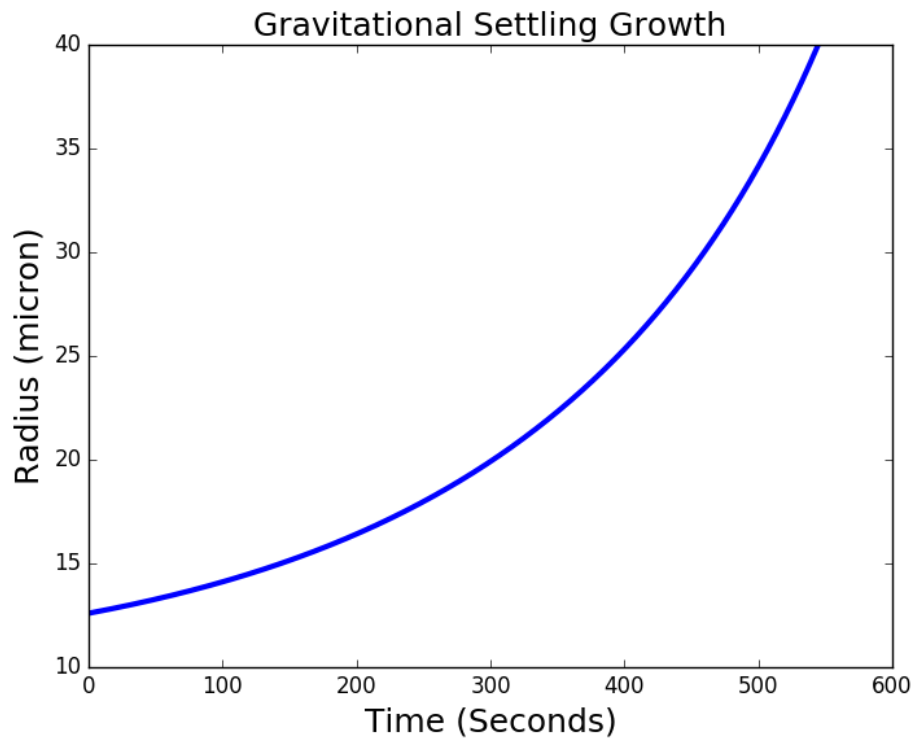

Figure 2.3: Time vs Radius plot for a droplet growing by gravitational settling from a radius of $12.6\,\mu$m to $40\,\mu$m. The initial growth is slow. The growth is obtained by solving equation 2.16 with $\epsilon = 1$.
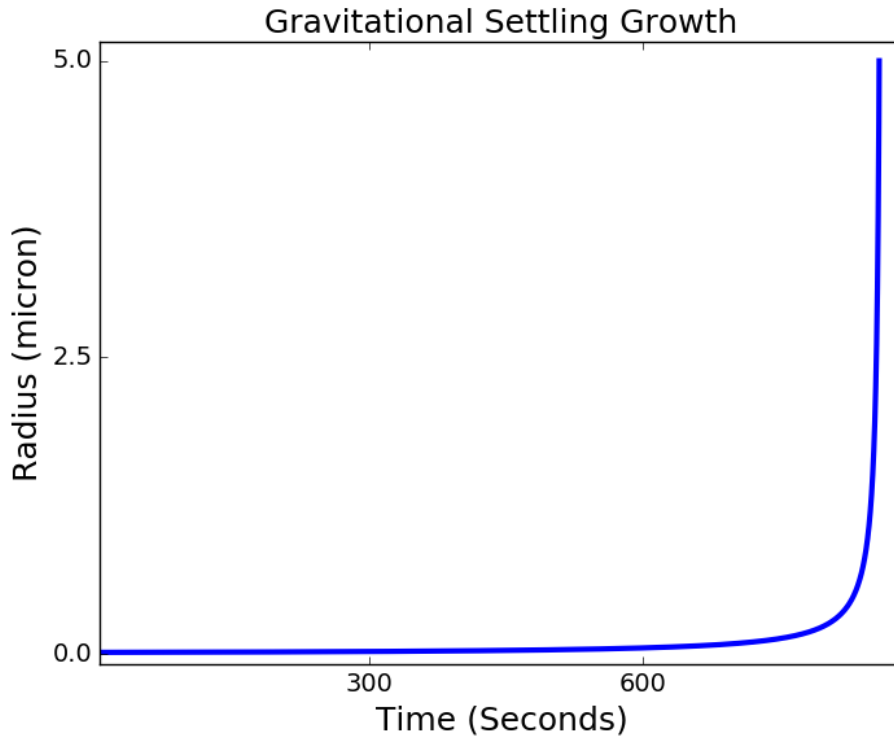
Figure 2.4: Time vs Radius plot for a droplet growing by gravitational settling from a radius of $12.6\,\mu m$ to $5\,mm$. The growth is rapid after the droplet reaches around $50\,\mu m$

2.5   Droplet Growth Bottleneck

The cloud droplet growth bottleneck is the failure to explain the rapidity of onset of warm rain. Warm rain is rain from a cloud that does not contain any ice while the onset of rain is when the cloud droplets grow large enough to fall as rain. Observations show that cloud droplets grow from 10 microns to 1 mm in about 10-15 minutes

Growth by condensation alone to a radius of around a millimetre, assuming constant ambient temperature and an infinite reserve of water vapour, would take several days as larger drops grow slower. Growth by gravitational settling alone would require over an hour, despite assuming high collision efficiency ($= 0.3$ initially, unity after droplet reaches $\approx 20\,\mu m$) of small droplets, assuming the droplet remains spherical throughout (large droplets will deform and take up a different shape) and assuming Stokesian terminal velocity throughout (Stokes drag is only a linear approximation to the drag

on a sphere, valid for very small drops).

Range	T_c	T_g
$10\,\mu m$ to $20\,\mu m$	1 to 2 mins	~ 1 hour
$20\,\mu m$ to $50\,\mu m$	20 to 30 mins	~ 10 mins
$50\,\mu m$ to $1\,mm$	3 to 4 days	$\sim 4mins$

Table 2.1: *Lowest time (ie. fastest) for a droplet to grow by condensation (T_c) and gravity (T_g) obtained by solving the respective growth equations. The simplifying assumptions include - assuming constant ambient temperature and supersaturation, assuming the upper bound on collision efficiency for the given range (from experimentally measured quantities) and assuming Stokes drag on the spherical droplet for terminal velocity.*

Until a size of about 10-12 microns, condensation growth occurs rapidly. However, once all the droplets are activated and reach this size, their growth due to condensation slows down for several reasons.

1. The growth rate of the radius of the droplet is inversely proportional to the radius.

2. The water vapour in the atmosphere is depleted due to condensation and this reduces the rate of condensation

3. Due to the contribution of heat by the condensation of water on to every droplet, the ambient temperature cannot be treated as constant. The temperature of the atmosphere rises as a result and this reduces the rate of condensation

4. In reality, each droplet is exposed to fluctuating temperature and water vapour. Thus while condensation occurs, evaporation occurs simultaneously for some droplets.

To reach from 10 microns to about a millimetre by gravitational settling requires, even under ideal conditions, a little over an hour. The growth from about 35-40 microns to a millimetre, under simplifying assumptions is rapid and only takes a few minutes.
A poor 10 micron droplet, 15 minutes later, almost magically, acquires immense water, grows and transforms and this parvenu eventually reaches the earth as a life-giving raindrop The gap between 10 microns to 40 microns is the fundamental gap in our understanding of cloud droplet growth and this is known as the cloud droplet growth bottleneck. The mechanism for the quick

onset of rain by this rapid growth of droplets by remains poorly understood and is the subject of much research and speculation. [3, 4]

Chapter 3

Fluid Dynamics

3.1 Introduction

The equation(s) describing the flow of a viscous, incompressible fluid is(are) the well-known incompressible Navier-Stokes Equation(s) given as follows

$$\partial_t \mathbf{u} + (\mathbf{u} \cdot \nabla)\mathbf{u} = -\nabla p + \nu \nabla^2 \mathbf{u} + \mathbf{f};$$
$$\nabla \cdot \mathbf{u} = 0. \tag{3.1}$$

where $\mathbf{u}$ is the velocity field of the fluid, t is time, p is the pressure, ν is the fluid kinematic viscosity and $\mathbf{f}$ a large scale forcing which is the energy input for the flow.

While finding exact, analytical solutions to the Navier-Stokes equations is a centuries old problem, it is possible to solve the equations numerically and this aspect will be discussed later.

3.2 Turbulence

An empirically observed ubiquitous characteristic of fluid flows is the development of turbulence. To define turbulence is not straightforward. It is (most often) a high Reynolds number ($Re = \frac{Ul}{\nu}$) phenomenon. U is a characteristic velocity of the flow, and l is a characteristic length. After onset of turbulence, the flow is no longer streamline and becomes chaotic and seemingly random. Turbulent flows show features of all length scales.

3.2.1 Energy Cascade

In an on-average steady flow, we can write the instantaneous velocity field as the sum of a time-averaged steady flow $\bar{\mathbf{u}}$ and an instantaneous perturbation

u'. **u'** is made of a collection of small vortices or eddies of a whole spectrum of sizes.

The dissipation of the kinetic energy (per unit time per unit mass) by viscosity of a fluid is $\epsilon = 2\nu S_{ij}S_{ij}$ where S_{ij} is the strain rate tensor given by $\frac{1}{2}(\partial u_i/\partial x_j + \partial u_j/\partial x_i)$. Dissipation is greater when velocity gradients are greater, thus the smallest eddies are the most dissipative. In a turbulent flow, we find eddies from the size of the order of the size of the flow (in other words, at the scale of the forcing that is driving the flow) to the smallest scale possible within the flow, which is the scale where the viscous dissipation completely dominates and all the energy is lost as heat. This smallest scale is known as the Kolmogorov length scale while the largest length scale, is known as the integral scale. [5]

Kolmogorov Microscales

According to the widely accepted Kolmogorov 1941 theory of turbulence, the smallest scales of turbulence, now know as the Kolmogorov microscales, depend only on ϵ, the average rate of kinetic energy dissipation per unit volume in the flow, and ν, the kinematic viscosity of the fluid. By pure dimensional analysis, we can set the smallest length and time scales respectively of the flow as

$$\eta = \left(\frac{\nu^3}{\epsilon}\right)^{\frac{1}{4}} ; \quad \tau_\eta = \left(\frac{\nu}{\epsilon}\right)^{\frac{1}{2}}$$

Energy transfer happens in turbulent flows through eddies. The largest eddies break-up to form smaller eddies, which further break-up, forming even smaller eddies until their energy is lost to viscosity at the Kolmogorov scale. This flow of kinetic energy from large scales to small scales is called the energy cascade. [6]

3.2.2 Intertial Range

There is an empirical law of turbulence that at large Re, the expected value of the square of the velocity difference of the fluid between two points separated by a distance l goes as $< (\delta l)^2 > \propto l^{\frac{2}{3}}$. This can be shown to be equivalent to saying that the energy spectrum follows $E(k) \propto k^{-5/3}$ where $E(k)$ is kinetic energy at length scale k.

This scaling law is observed in experiments over a large range of length scales called the intertial range. The intertial range may be said to be the length scales significantly smaller than the integral scale and significantly larger than the Kolmogorov scale.

3.3　Particles in a Flow

When particles are in a fluid, they respond to the flow of the fluid via a drag force and are thus transported by the fluid. The dynamics of inertial particles depend on their characteristic time scale $\tau_p = \frac{2a^2\rho_p}{9\nu\rho_f}$, characterised by the dimensionless Stokes number $St = \tau_p/\tau_\eta$, where τ_η is the Kolmogorov time-scale associated with the flow. ρ_p and rho_f are the density of the particle and the fluid respectively.

　　The equation of motion for a single spherical particle is obtained by integrating over the surface of the particle the stresses acting on the particle, for which we obtain [7]

$$\rho_p \frac{d\mathbf{v}}{dt} = \rho_f \frac{D\mathbf{u}}{Dt} + (\rho_p - \rho_f)\mathbf{g} \quad -\frac{9\nu\rho_f}{2a^2}\left(\mathbf{v} - \mathbf{u} - \frac{a^2}{6}\nabla^2\mathbf{u}\right) \quad -\frac{\rho_f}{2}\left(\frac{d\mathbf{v}}{dt} - \frac{D}{Dt}\left[\mathbf{u} + \frac{a^2}{10}\nabla^2\mathbf{u}\right]\right).$$
$$(3.2)$$

　　Under the conditions of our interest of dilute suspensions, small droplets ($a << \eta$), negligible buoyancy and $\rho_p \gg \rho_f$, this equation simplifies greatly to,

$$\frac{d\mathbf{x}}{dt} = \mathbf{v};$$
$$\frac{d\mathbf{v}}{dt} = -\frac{\mathbf{v} - \mathbf{u}}{\tau_p} \qquad (3.3)$$

3.3.1　Preferential Concentration of Particles

Q-criterion

While the concept of vortex in fluid dynamics is well understood intuitively, there is no universally accepted, rigorous definition for a vortex. It is, generally, a region of high vorticity. (Vorticity is defined as the curl of the fluid velocity field) Highly rotational regions are associated with regions of high vorticity.

The Q-criterion was introduced by Hunt, Wray and Moin (1998) to define regions of high vorticity. First, we write the velocity gradient tensor V_{ij} as $V_{ij} = \frac{\partial u_i}{\partial x_j}$. Every second order tensor can be expressed as the sum of a symmetric and an anti-symmetric tensor.

$$V_{ij} = R_{ij} + S_{ij}$$

where

$$S_{ij} = \frac{1}{2}\left(\frac{\partial u_i}{\partial x_j} + \frac{\partial u_j}{\partial x_i}\right)$$

18

is the symmetric tensor and

$$R_{ij} = \frac{1}{2} \left(\frac{\partial u_i}{\partial x_j} - \frac{\partial u_j}{\partial x_i} \right)$$

is the anti-symmetric part.

Q is defined as

$$Q = \frac{1}{2} \left[\mid R \mid^2 - \mid S \mid^2 \right]$$

The Q-criterion defines a vortex as a region with $Q > 0$. $\mid R \mid^2$ and $\mid S \mid^2$ can be interpreted as the degree of rotation and strain in the flow respectively. Vortical regions are where the rotationality of the flow dominates over the strain while non-vortical regions, or stretching regions are regions where the straining nature of the flow dominates.

Preferential Concentration

When particles following the simplified Maxey-Riley equation (3.3) are suspended passively in a fluid, they tend to preferentially cluster in regions of low vorticity, corresponding to regions of high strain. Thus, particles are evacuated from highly rotational (R dominated) regions of the flow. This phenomenon can be understood as being caused the finite relaxation time of the particle.

From equation (3.3), it is apparent that τ_p is a timescale for the particle to respond to the flow (hence τ_p is known as the particle response time). When τ_p tends to zero, the numerator also tends to zero. Thus, particles with very small τ_p behave like "tracer particles", which follow the flow exactly.

The non-tracer behaviour of finite size, inertial particles is thus a consequence of the finite response time to the flow. In highly rotational regions, the particles thus experience a sling action and are thrown out of vortices. In weaker rotation regions, the particles are still ejected from the vortex, but more passively, until the particles reach a more quiescent region of the flow. [8]

Simulations conducted by Dr. Jason R Picardo at ICTS in conjunction with this study also indicate that particles initially in regions of higher vorticity are ejected out of vortices far more rapidly than particles in regions of lower vorticity. This fact will be revisited later in the discussion of the results and potential applicability of the work described in this thesis.

3.4 Computational Fluid Dynamics

A program to solve the incompressible Navier-Stokes equation for statistical, homogeneous and isotropic turbulence was designed by Dr. Samriddhi Sankar Ray at ICTS. It uses the Galerkin approach to solving the Navier-Stokes equation. (3.1) can be written in Fourier Space as

$$\left(\frac{d}{dt} + \nu \mid \mathbf{k} \mid^2\right) \hat{\mathbf{u}}_{\mathbf{k}} = -i\mathbf{k}\hat{\mathbf{p}}_{\mathbf{k}} - (\widehat{\mathbf{u} \cdot \nabla \mathbf{u}})_{\mathbf{k}} + \mathbf{f}_{\mathbf{k}} \qquad (3.4)$$

$$i\mathbf{k} \cdot \hat{\mathbf{u}}_{\mathbf{k}} = \mathbf{0} \qquad (3.5)$$

The pressure term p is eliminated by taking $i\mathbf{k}$ and dotting with (3.4) and then using (3.5). Thus, we get

$$\left(\frac{d}{dt} + \nu \mid \mathbf{k} \mid^2\right) \hat{\mathbf{u}}_{\mathbf{k}} = \hat{\mathbf{c}}_{\mathbf{k}} - \mathbf{k}\frac{\mathbf{k} \cdot \hat{\mathbf{c}}_{\mathbf{k}}}{\mid \mathbf{k} \mid^2} + \mathbf{f}_{\mathbf{k}} \qquad (3.6)$$

where $\hat{\mathbf{c}}_{\mathbf{k}} = -(\widehat{\mathbf{u} \cdot \nabla \mathbf{u}})_k$. The Galerkin approach, or the Fourier Galerkin approximation, as it is known, involves terminating the sum of Fourier modes at $\mid k_1 \mid, \mid k_2 \mid, \mid k_3 \mid, < N/2$. N is the number of grid points taken over the computational domain, appropriately chosen to resolve the Kolmogorov scale. This is done as viscous dissipation doesn't allow persistence of any structures below this length scale. [9]

For the Fourier transforms, a Fast Fourier Transform package is used while the code is solved 'pseudo-spectrally'. The pseudo-spectral method involves performing multiplication operations in real space and derivates in Fourier space, since the derivatives reduce to a simple multiplication in the latter.

Chapter 4

Turbulence in Clouds

4.1   Is Turbulence the Answer?

One of the dominant ideas among cloud physicists to solve the cloud droplet bottleneck is that turbulence in clouds significantly enhances the number of collisions between droplets and thus accelerates the creation of large drops. [3]

After all, as discussed previously, in turbulent flows, particles cluster in regions of low vorticity, increasing the local density of particles and thus increasing the likelihood of collisions. Additionally, collisions between particles occur when there exist large gradients in the flow to bring particles together. Turbulent flows abound with large velocity gradients.

To be noted is the central fact that the enhancement of collision rates need not be great for the cloud system to evolve rapidly. Approximately one in a million droplets undergoing runaway growth can trigger formation of raindrops.

4.1.1   Caustics Collisions and Vortices

The rate of collisions between particles suspended in turbulent flows is well studied and there exist several studies exploring this particular question. Recent studies have also, in particular, pointed to the collisions caused by rapid ejection of particles from strong vortices.

When particles are in a strong vortex (region of high Q), they are ejected out rapidly. This is known as the sling effect. Such rapidly ejected particles can be the seed for multiple collisions upon exiting the vortical region and meeting several particles in a more quiescent region of the flow, outside the vortex. This is a meeting of two particles with vastly different trajectories

and flow histories. Such a situation, where particles are highly decorrelated from the flow and multiple particles arrive at the same point with very different velocities is known as caustics. This means that a "field description" of the particle density is not valid. [4]

4.2 Vortices in 3D Turbulence
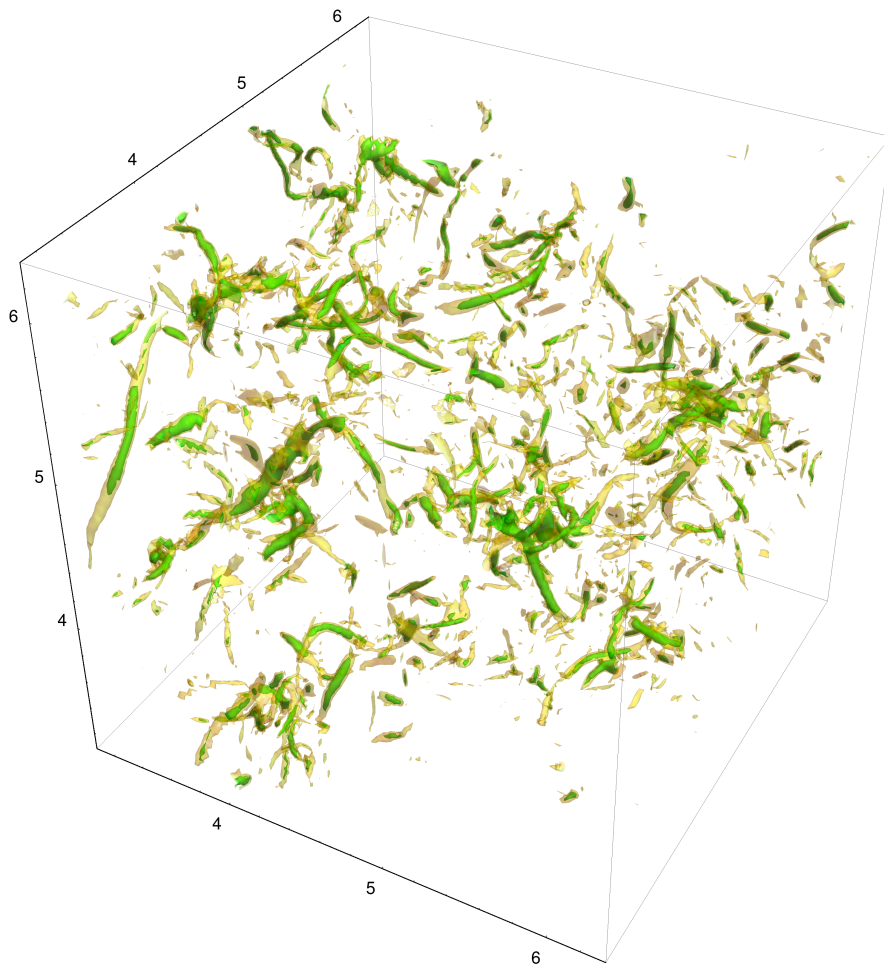
Figure 4.1: Contours of regions with vorticity above a certain value. Coloured regions have vorticity higher than the cut-off vorticity of $\sqrt{\langle \omega^2 \rangle \mathrm{Re}}$. Simulation performed by Dr. Jason Picardo at ICTS, Bengaluru.

The fundamental limitation of exploring the role of vortices (and turbulence in general) is the finite availability of computational resources. The mea-

sured Reynolds number of cloud turbulence can be as high as 10000 while computational resources rarely allow simulations to achieve such high values. A cut-off vorticity of $\sqrt{\langle \omega^2 \rangle \mathrm{Re}}$ is often used to to define regions of high vorticity in a turbulent flow. Empirical studies of turbulent simulations have shown that such regions of high vorticity in turbulent flows are organised into thin tube-like vortical structures (see fig 4.1) with a small radius ($\approx 5\eta$, where η is the Kolmogorov length scale) compared to the length of the tube-like vortical structure ($\approx L$, where L is the integral length scale). [10]

4.3   The Burgers Vortex

A simple way to explore the role of vortices in enhancing collisions is to independently study collisions around a stand-alone, model vortex, which can be used to understand how collisions occur near vortices and to then verify if similar behaviour is observed in actual turbulence simulations and experiments.

The Burger's vortex is a cylindrically symmetric vortex flow. It has been shown that it very accurately models a tubular vortex, typical of the kind seen in turbulent flows. The vorticity is maximum at the centre and falls off with exponentially with increasing distance from the centre of the cylinder about which the vortex is symmetric. The velocity flow field is given by

$$V_\theta = \frac{\Gamma}{2\pi r}\left(1 - \exp(-\frac{r^2}{r_v^2})\right);$$

$$V_r = \sigma r; \quad V_z = 2\sigma z \tag{4.1}$$

Γ is the circulation of the vortex, r_v is a characteristic radius and σ is known as the stretching co-efficient, which induces a stretching flow outward along the z-axis and radially inward. [5]
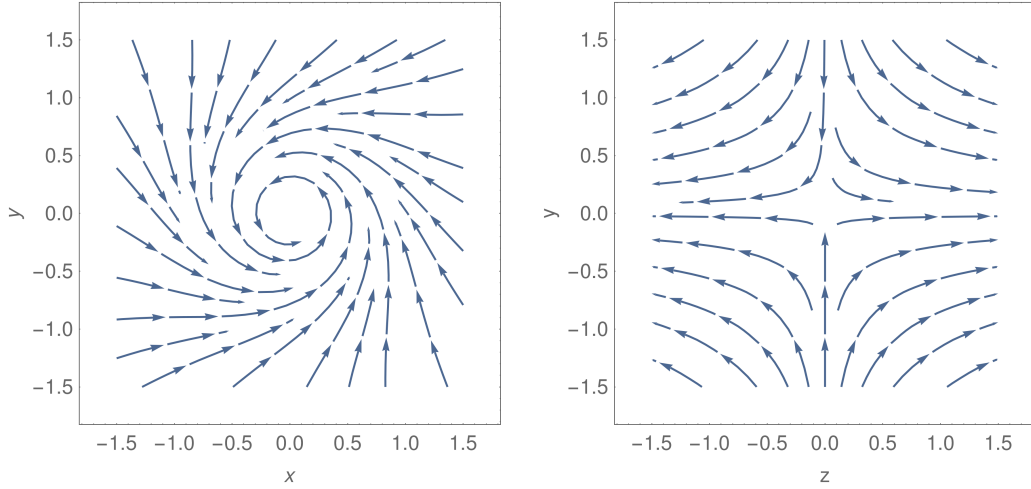
Figure 4.2: The flow-field of the Burgers vortex in the radial and axial directions. The radial flow features a rotational flow while the axial flow is a stretching flow.

4.4   Collisions Around a Burgers Vortex

The main results of this study concern the particle trajectories and collisions around a Burgers vortex. Since the vorticity of the Burgers flow is maximum at the centre and decreases as we move away from the centre, particles closer to the centre of the vortex are ejected much faster than particles that are further away from the centre. This causes collisions in multiple ways

1. Particles initially at different distances from the centre can collide as the inner droplet will overtake the outer droplet during ejection from the region of high vorticity.

2. On rapid ejection from the region of high vorticity, the particle can collide successively with relatively quiscent droplets outside the core of the vortex

3. The ejection from vortices increases the local density of droplets away from the centre of the vortex, thus making collisions more likely.

Previous studies on 2-D Burgers vortices (only radial) showed that characteristic length for the Burgers vortex, known as the "caustics radius" (r_c), given by $0.55\sqrt{\Gamma\tau_p}$ (See [11]). For the "caustics collisions", that is collisions of the

type 1, we need the vortex radius to be smaller than the caustics radius, ie. $r_v < r_c$. [11, 12]

4.4.1   Simulation of Burgers Vortex

To understand how particles behave near a Burgers vortex, a code was written by the author that simulated a system of uniformly distributed particles, initialised around a Burgers flow field. The particles followed the simplified Maxey-Riley equation (3.3) and the flow-field was stationary.
The parameters were set to model cloud turbulence as closely as possible, using measured parameters. To do this, the Burgers vortex parameters were chosen to model a typical tubular, strong vortex in cloud turbulence.
The parameters chosen were

$$\nu = 1.48 \times 10^{-5}\,\mathrm{m^2\,s^{-1}} \qquad \epsilon = 0.2\mathrm{m^2\,s^{-3}} \qquad \mathrm{St} = 0.01$$

Here, ν is the kinematic viscosity of air, ϵ is the energy dissipation per unit volume per unit time and St is the ratio of the particle relaxation time τ_p to the Kolmogorov fluid time scale τ_η. The Stokes number of 0.01 is typical of small cloud droplets of the sizes of our interest. Specifying ϵ and ν automatically set the Kolmogorov length scale and the time scale, η and τ_η respectively.
Thus, we get the typical radius of the vortex to be of the order of $r_v \approx 5\eta$. To set the circulation, we consider the well-known result that $\langle \omega^2 \rangle = \frac{2\epsilon}{\nu}$, where the expectation value represents an average over space and consider the above mentioned high-vorticity cut-off as a typical value for the vorticity of the model vortex.
The dimension of vorticity 'ω' is $\mathrm{m\,s^{-1}}$. Thus, using the typical vorticity of a strong vortex defined by the cut-off in the above paragraph, we can elicit a typical velocity scale by purely dimensional arguments, using

$$\omega = \frac{u}{l}$$

Here l is given by 5η and ω is given by

$$\sqrt{\langle \omega^2 \rangle \mathrm{Re}}$$

and

$$\langle \omega^2 \rangle = \frac{2\epsilon}{\nu}$$

Having obtained the velocity scale of such a typical vortex, we can define a typical circulation by $\Gamma = ul$ using dimensional arguments.

The stretching coefficient σ is given by $\sigma = \frac{4\nu}{l^2}$ (see [5], page 250).
Using these parameters, we get, in appropriately scaled coordinates to make the numbers more computationally tractable,

$$\Gamma = 36.7; \ \ r_v = 0.2; \ \ \sigma = 0.16; \ \ r_c \approx 0.3$$

To compare this with a less intense vortex, we consider another vortex with $l = 10\eta$ and an appropriate value for sigma according to the formula above. Such a vortex has $r_v = 0.4$ in our working units. Such a vortex has a lower vorticity at the centre of the vortex and the vorticity falls off much slower compared to the original vortex. We will hence forth refer to the more intense vortex ($r_v = 0.2$) as the "thin vortex" while referring to the less intense vortex ($r_v = 0.4$) as the "wide vortex". The particles were taken to be larger than actual cloud droplets to obtain large number of collisions and thus better understand the statistics of collisions.

Particles Around the Vortex

200000 particles are initialised with the same velocity as fluid in a 4 X 4 X 4 box around the centre of the vortex. These particles are allowed to evolve according to equation (3.3) and collisions between the particles are detected explicitly using a collision detection routine designed by the author, similar to the collision detection algorithm of Sundaram and Collins [13]. This is run for a short time, corresponding to $0.1\tau_\eta$. This is to account for the fact that a real flow is constantly changing. Though tubular vortices are often known to last far longer, in the interest of keeping the model realistic, the run time was restricted to a fraction of τ_η.
The collisions were studied for both, the thin vortex as well as the wide vortex. The simulation was performed with a monodisperse spectrum of particles as well as a polydisperse spectrum of particles. (Dispersity refers to the distribution of their radii. A monodisperse spectrum of particles have equal radii and a polydisperse spectrum of particles have particles of different radius). The mean radii for both spectra were the same, while the radii for the polydisperse spectrum followed a Gaussian distribtion with a small standard deviation of 10% of the mean.
Additionally, every time a collision was detected between two droplets, the droplets were coalesced to form a larger droplet with the total mass and momentum from the two droplets being conserved.
The results from these simulations are presented below in 4 plots. These plots are the average over an ensemble of 50 runs.

4.5 Collisions Around a Burgers Vortex
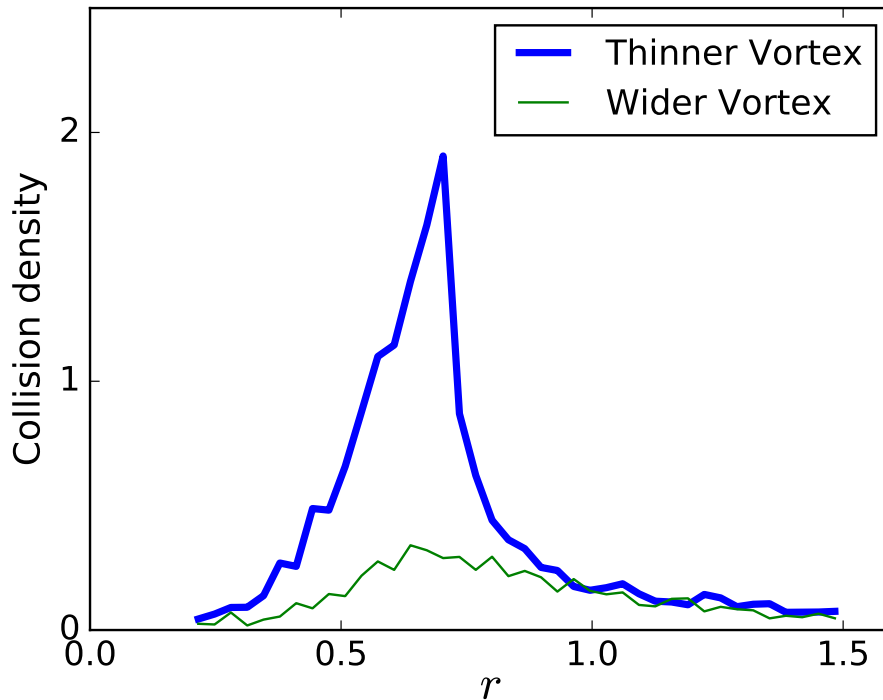
Figure 4.3: A plot of collision density (Average No. of collisions per unit volume in the run-time) vs radius r where the collision occurs. This shows a clear, localised spike in the number of collisions outside the "vortex core" region for the thin vortex, where particles are ejected out strongly. For the wide, less intense vortex, a similar spike is not seen as particles are not ejected as rapidly from the vortex, though a small spike is seen. This is indicative that the caustics radius picture is valid for 3D as well.

Further simulations showed that the stretching and 3D nature of the model serves only to increase the number of collisions, while the qualitative nature of the collisions with respect to the radius at which collisions occur remains nearly the same. For this purpose, a comparison was carried out with a Burgers vortex with $\sigma = 0$, which is analogous to the 2D vortices studied in [11] and [12], a plot of which is shown below.
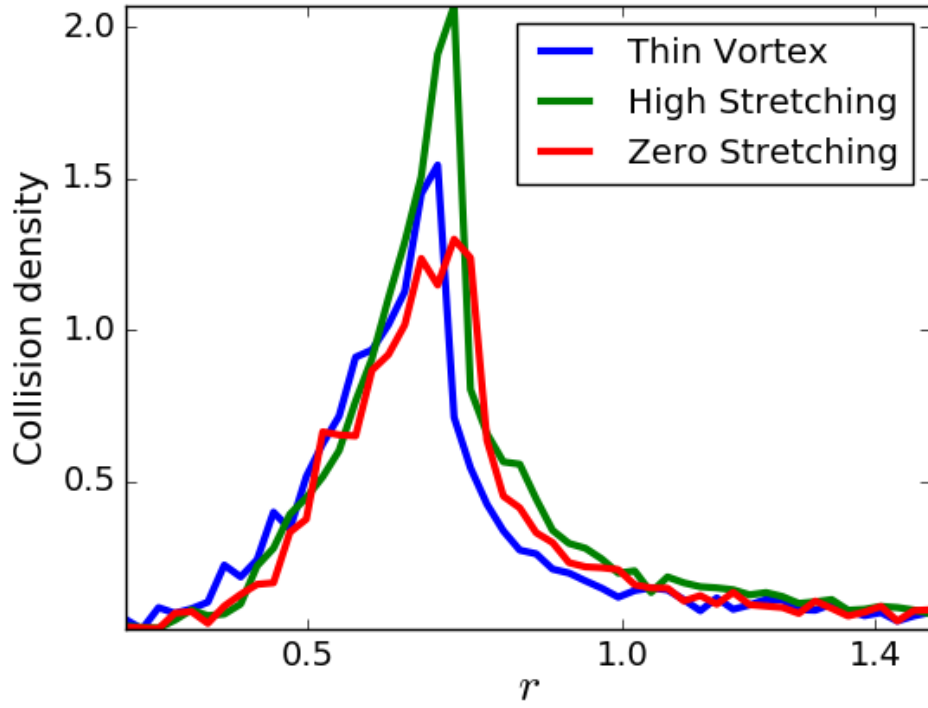
Figure 4.4: A plot of collision density for the same vortex radius ($r_v = 0.2$) and circulation ($\Gamma = 36$) with different values of the strain rate σ. We have $\sigma = 0$ (Zero Stretching), $\sigma = 0.16$ (Thin Vortex) and $\sigma = 0.5$ (High stretching) for comparison. It is clear that the stretching only enhances the number of collisions and does not add other significant dynamic effects
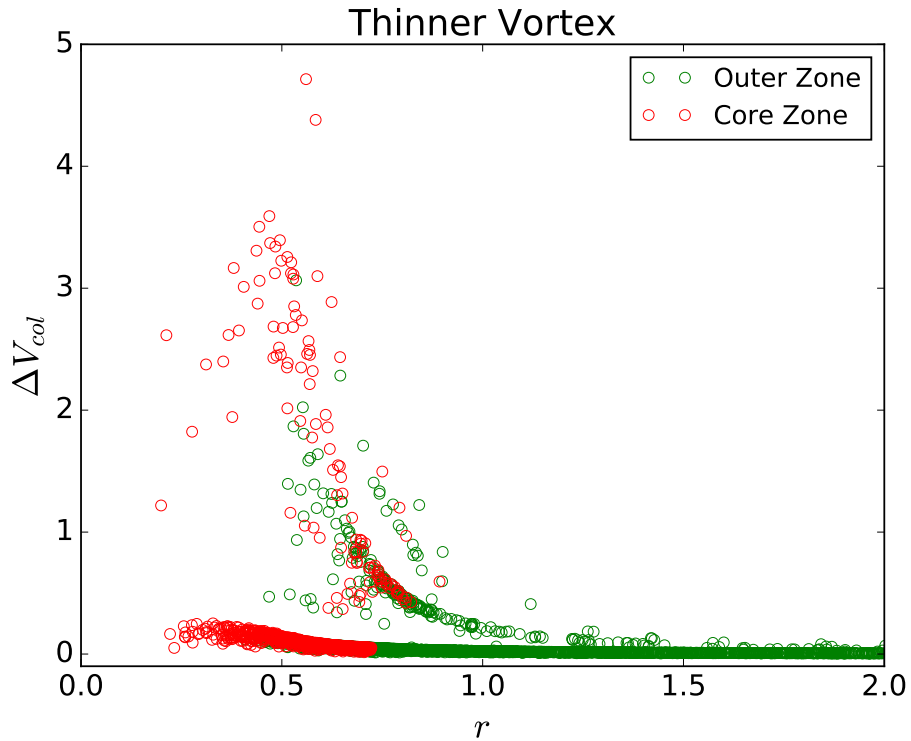
Figure 4.5: A plot of the absolute relative velocity of collision against the radius at which the collision occurred. Each data point represents a collision. If either of the particles involved in the collision originated from within the core region ($r < 0.35$), the point is coloured red. Else, it is coloured green. It is clear that almost all "high relative velocity collisions" involve at least one particle from within the core region. Also, all the collisions occurring up to a radius ≈ 0.7 are coloured red, thus involving droplets from the core region. This is compatible with the model that the chief cause for collisions is the ejection of particles from the core of the vortex in a sling action.
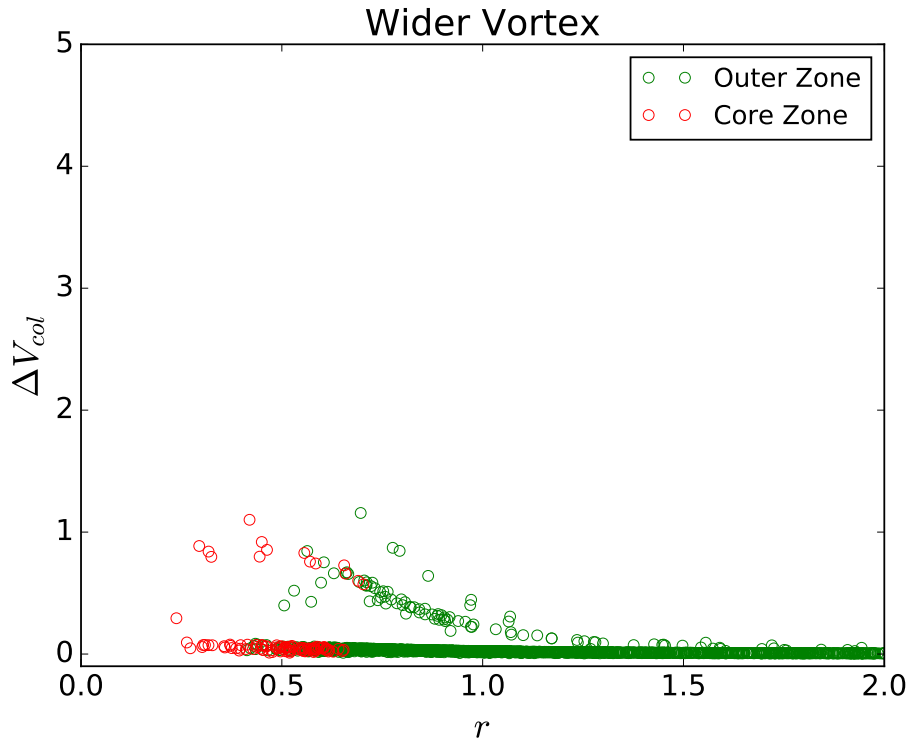
Figure 4.6: A plot of the absolute relative velocity of collision against the radius at which the collision occurred. Each data point represents a collision. If either of the particles involved in the collision originated from within the core region ($r < 0.35$), the point is coloured red. Else, it is coloured green. The first point to note is the lack of relatively high relative velocity collisions compared to Figure 4.2. In addition, the "red collisions" involving droplets from within the core region of the droplet dominate collisions up to a much smaller distance from the centre. Here, it indicates that the wider, less intense vortex does not eject particles as strongly as the more intense vortex.
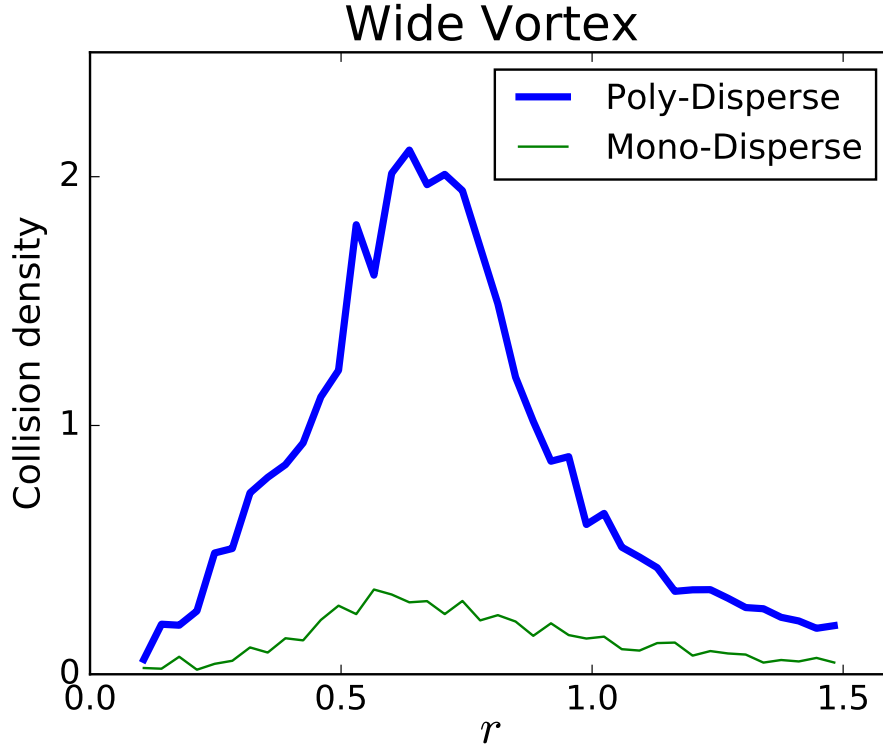
Figure 4.7: A plot of collision density vs radius of collision comparing the collision characteristics of the polydisperse spectrum with that of the monodisperse spectrum in the wide vortex. Due to differences in size, the particles respond differently to the flow according to equation (3.3). This lends itself to more collisions in all regions of the flow and the number of collisions for even a less intense vortex is vastly enhanced due to polydispersity. In reality, cloud droplets are in fact polydisperse, thus very strong vortices aren't necessary to have a large number of collisions.

4.5.2 Large Droplets

To further understand the origin of colliding droplets, all droplets initially within the caustics radius ($r_c \approx 0.3$) were initially tagged with '1' while droplets outside initially outside this cylinder of radius r_c were tagged with '0'. Simultaneously, the same number of random droplets were given a second tag of '0' and '1' respectively. (That is, if there were initially n droplets within the caustics radius numbered '1', then n randomly taken droplets were also tagged '1' and similarly with the number of droplets outside the caustics radius). At every coalescence, the tag of the resulting droplet was given the value of the sum of the tags of the two colliding droplets.

At the end of the monodisperse run, the tag of the larger particles (particles

that had undergone at least one collision) were considered. The particles with tags greater than one, that is, particles with at least one component from within the core region, were counted and compared with the same number of particles, randomly distributed across the domain by counting the second tags of the large droplets as well.

For the thin vortex, the ratio of number of large droplets originating from within the caustics radius to the number of large droplets originating from a randomly tagged set of droplets was 2.86, while the same ratio for the wide vortex was 0.15. This demonstrates clearly, the disproportionate participation of particles close to the vortex centre in collisions and is highly indicative of collisions occurring due to ejection of vortices.

Chapter 5

Discussion and Future Work

The above results regarding a Burgers vortex are promising. It is clear that in a Burgers vortex in isolation, the mechanism of evacuation of vortices and clustering of particles in non-vortical regions leads to an enhancement in collisions. The large number of high relative velocity collisions in the region just outside the core of the vortex and the disproportionate presence of particles from the core region in collisions clearly demonstrates the same.

However, one must exercise a great deal of caution before staking any general claims regarding the direct role of vortices in enhancing collisions in a turbulent flow for several reasons. The Burgers vortex is a static flow-field modeling a dynamic flow field. It is possible that the dynamics of a tube-like vortex, even within its life-span, can dominate the properties of the vortex and this dynamics is not captured by a simplistic measure used to visualise the vortices. In addition, the fraction of volume occupied by such structures in a turbulent flow-field and the frequency of their occurrence is subject to much uncertainty. It is known empirically that with increasing Reynolds number, the frequency of "extreme events", such as instances of very strong and long-lived vortices, increases. This is known as intermittency and is a fundamental property of turbulent flow-fields, but there are no exact scaling laws to quantify the same for Reynolds numbers as high as those seen in clouds. [5]

Simulations of 3D turbulence using the pseudo-spectral method described in Section 3.4 are currently underway at ICTS, with location of collisions of inertial particles, among other things, being investigated by Dr. Jason Picardo. For this, the same collision detection routine written by the author is being used and there is promising head-way made on the question of vortices and collisions. Two early results are highlighted qualitatively here

1. The number of collisions outside regions of high vorticity is disproportionately larger than can be explained only by preferential concentra-

tion. It could be that the disproportionately large number of collisions arise from particles being ejected out of vortices and participating in collisions in a Burgers-like mechanism.

2. The time for a particle to leave a vortical region is inversely proportional to the strength of the local vorticity when it is ejected. In other words, a particle in a region of larger vorticity reaches a region of low vorticity faster than a particle in a region of lower vorticity leaves the vortical region and enters a region of low vorticity. This suggests that strong evacuation of vorticity is a reality and particles closer to the "core" regions of vorticity are in fact thrown out rapidly in such a way that they can overtake the particles which are a little away from the local maxima of vorticity.

While neither of these results is conclusive on the role vortices play in enhancing collisions in turbulent flows, they are certainly not incompatible with the Burgers-like ejection mechanism as a source of large number of collisions in turbulence. They are, one could argue, quite indicative of the same. Simulations are being carried out currently and perhaps more data from these simulations can lend more hints on the exact mechanism for collisions in turbulence and how much of a role vortices have to play.

If vortices play a significant role in enhancing collisions, there are several potential implications. Most significantly, it could provide a simple way to scale-up results from simulations of relatively low Reynolds number turbulence to cloud turbulence as it would only require a study on the nature and frequency of vortices in cloud turbulence to understand the collision rates in clouds. A better understanding of how cloud droplets grow is central to solving several problems related to the representation of clouds in General Circulation Models, which model Global Climate. The dynamic effects of clouds on atmospheric circulations and their feedback on to global climate remains the least understood aspect of global climate models.

Further work being carried out currently by the author includes understanding the exact trajectory of particles in a Burgers vortex, understanding the effect of gravity on collisions in the Burgers vortex system and looking for more clues from the simulations of 3D turbulence. Since working codes have been built for both, the Burgers vortex and 3D turbulence and significant experience in running these simulations has been garnered over the course of this study, the scope for future work is promising and one can (in the humble opinion of the author) afford to be optimistic about the same.

References

[1] R. R. R. M.K. Yau, A Short Course in Cloud Physics, 3rd Edition, International Series in Natural Philosophy, Butterworth-Heinemann, 1996.

[2] J. K. H.R. Pruppacher, Microphysics of Clouds and Precipitation, 2nd Edition, Atmospheric and Oceanographic Sciences Library, Springer, 1996.

[3] W. W. Grabowski, L.-P. Wang, Growth of Cloud Droplets in a Turbulent Environment, Annual Review of Fluid Mechanics 45 (1) (2013) 293–324. `doi:10.1146/annurev-fluid-011212-140750`.
URL `http://www.annualreviews.org/doi/10.1146/annurev-fluid-011212-140750`

[4] A. Pumir, M. Wilkinson, Collisional Aggregation Due to Turbulence, Annual Review of Condensed Matter Physics 7 (1) (2016) 141–170. `arXiv:1508.01538`, `doi:10.1146/annurev-conmatphys-031115-011538`.
URL `http://www.annualreviews.org/doi/10.1146/annurev-conmatphys-031115-011538`

[5] P. A. Davidson, Turbulence: An Introduction for Scientists and Engineers, Oxford University Press, USA, 2004.

[6] U. Frisch, Turbulence, the legacy of A.N. Kolmogorov, Cambridge University Press, 1995.

[7] M. R. Maxey, Equation of motion for a small rigid sphere in a nonuniform flow, Physics of Fluids 26 (4) (1983) 883. `arXiv:arXiv:1011.1669v3`, `doi:10.1063/1.864230`.
URL `http://scitation.aip.org/content/aip/journal/pof1/26/4/10.1063/1.864230`

[8] J. K. Eaton, J. R. Fessler, Preferential concentration of particles by turbulence, International Journal of Multiphase Flow 20 (SUPPL. 1) (1994)

169–209. `arXiv:arXiv:1011.1669v3`, `doi:10.1016/0301-9322(94)90072-8`.

[9] A. Q. T. A. Z. Claudio G Canuto, M. Yousuff Hussaini, Spectral methods: evolution to complex geometries and applications to fluid dynamics, 1st Edition, Scientific Computation, Springer, 2007.

[10] J. Jiménez, A. a. Wray, On the characteristics of vortex filaments in isotropic turbulence, Journal of Fluid Mechanics 373 (1998) 255–285. `doi:10.1017/S0022112098002341`.

[11] S. Ravichandran, R. Govindarajan, Caustics and clustering in the vicinity of a vortex, Physics of Fluids 27 (3). `arXiv:1503.06919`, `doi:10.1063/1.4916583`.

[12] P. Deepu, S. Ravichandran, R. Govindarajan, Caustics-induced coalescence of small droplets near a vortex, Physical Review Fluids 2 (2) (2017) 1–12. `doi:10.1103/PhysRevFluids.2.024305`.

[13] S. SUNDARAM, L. R. COLLINS, Collision statistics in an isotropic particle-laden turbulent suspension. Part 1. Direct numerical simulations, Journal of Fluid Mechanics 335 (1997) S0022112096004454. `doi:10.1017/S0022112096004454`.
URL `http://www.journals.cambridge.org/abstract{_}S0022112096004454`